

Exact-exchange energy density in the gauge of a semilocal density functional approximation

Jianmin Tao

Theoretical Division, Los Alamos National Laboratory, Los Alamos, New Mexico 87545, USA

Viktor N. Staroverov

Department of Chemistry, University of Western Ontario, London, Ontario N6A 5B7, Canada

Gustavo E. Scuseria

Department of Chemistry, Rice University, Houston, Texas 77005, USA

John P. Perdew

*Department of Physics and Quantum Theory Group,
Tulane University, New Orleans, Louisiana 70118, USA*

(Dated: October 22, 2018)

Exact-exchange energy density and energy density of a semilocal density functional approximation are two key ingredients for modeling the static correlation, a strongly nonlocal functional of the electron density, through a local hybrid functional. Because energy densities are not uniquely defined, the conventional (Slater) exact-exchange energy density $e_x^{\text{ex(conv)}}$ is not necessarily well-suited for local mixing with a given semilocal approximation. We show how to transform $e_x^{\text{ex(conv)}}$ in order to make it compatible with an arbitrary semilocal density functional, taking the nonempirical meta-generalized gradient approximation of Tao, Perdew, Staroverov, and Scuseria (TPSS) as an example. Our additive gauge transformation function integrates to zero, satisfies exact constraints, and is most important where the density is dominated by a single orbital shape. We show that, as expected, the difference between semilocal and exact-exchange energy densities becomes more negative under bond stretching in He_2^+ and related systems. Our construction of $e_x^{\text{ex(conv)}}$ by a resolution-of-the-identity method requires uncontracted basis functions.

PACS numbers: 31.15.Ew, 71.15.Mb

I. INTRODUCTION

In Kohn-Sham density functional theory [1, 2], the exchange-correlation (xc) energy E_{xc} must be approximated as a functional of the electron spin-densities $n_{\uparrow}(\mathbf{r})$ and $n_{\downarrow}(\mathbf{r})$. This functional can be always written as

$$E_{\text{xc}}[n_{\uparrow}, n_{\downarrow}] = \int d\mathbf{r} e_{\text{xc}}(\mathbf{r}), \quad (1)$$

where $e_{\text{xc}}(\mathbf{r}) = n(\mathbf{r})\varepsilon_{\text{xc}}(\mathbf{r})$ is the exchange-correlation energy density, $n = n_{\uparrow} + n_{\downarrow}$ is the total electron density, and ε_{xc} is the exchange-correlation energy per electron. Approximations to $\varepsilon_{\text{xc}}(\mathbf{r})$ can be constructed in a fairly systematic way [3, 4] by employing increasingly complex ingredients built from the Kohn-Sham orbitals. Most of the existing exchange-correlation approximations use only ingredients found from the occupied Kohn-Sham orbitals at \mathbf{r} or in an infinitesimal neighborhood of \mathbf{r} , such as $n_{\sigma}(\mathbf{r}) = \sum_i^{\text{occ.}} |\phi_{i\sigma}(\mathbf{r})|^2$, $\nabla n_{\sigma}(\mathbf{r})$, and $\tau_{\sigma} = \frac{1}{2} \sum_i^{\text{occ.}} |\nabla \phi_{i\sigma}(\mathbf{r})|^2$, where $\sigma = \uparrow, \downarrow$. Such functionals are called semilocal and include the local spin density approximation [1, 5, 6], the generalized gradient approximation (GGA) [7], and the meta-GGA [8].

Semilocal functionals are often accurate [9, 10, 11, 12, 13] but tend to make large errors for open systems of fluctuating electron number [14, 15, 16, 17, 18], such as

fragments connected by stretched bonds. This occurs because semilocal functionals respect the exact hole sum rule for a closed system but not for an open one of fluctuating electron number [19], where (after symmetry breaking) the semilocal exchange typically overestimates the magnitude of the static correlation. We have argued [19] that, in order to correct these errors, one needs to go beyond the semilocal approximation and incorporate a fully nonlocal ingredient, the exact-exchange (ex) energy density $e_x^{\text{ex}}(\mathbf{r})$ conventionally (conv) defined as

$$e_x^{\text{ex(conv)}}(\mathbf{r}) = -\frac{1}{2} \sum_{\sigma=\uparrow,\downarrow} \int d\mathbf{r}' \frac{|\gamma_{\sigma}(\mathbf{r}, \mathbf{r}')|^2}{|\mathbf{r} - \mathbf{r}'|}, \quad (2)$$

where $\gamma_{\sigma}(\mathbf{r}, \mathbf{r}')$ is the one-electron σ -spin density matrix of the Kohn-Sham reference system

$$\gamma_{\sigma}(\mathbf{r}, \mathbf{r}') = \sum_i^{\text{occ.}} \phi_{i\sigma}(\mathbf{r}) \phi_{i\sigma}^*(\mathbf{r}'). \quad (3)$$

In the Jacob's ladder classification of density functional approximations [3], functionals that employ $e_x^{\text{ex}}(\mathbf{r})$ are called hyper-GGAs. We have also argued that a hyper-GGA can simultaneously achieve good accuracy and satisfy important exact constraints if the exact-exchange energy density is combined with a semilocal (sl) exchange-correlation in a so-called local hybrid (lh) functional

$$e_{\text{xc}}^{\text{lh}} = e_x^{\text{ex}} + [1 - a(\mathbf{r})](e_x^{\text{sl}} - e_x^{\text{ex}}) + e_c^{\text{sl}}, \quad (4)$$

where $0 \leq a(\mathbf{r}) \leq 1$ is the position-dependent mixing function. If $a(\mathbf{r}) = \text{const}$, Eq. (4) reduces to a global hybrid (gh) functional [20]. The general local hybrid form was suggested by Cruz *et al.* [21] as early as 1998, but specific forms of $a(\mathbf{r})$ were not proposed until later [3, 22]. The fundamental physical justification for local hybrids has been advanced only recently [19]. The local hybrid approach is, of course, not the only way of attacking the static correlation problem. Other distinct approaches are being actively pursued [23, 24].

When $a(\mathbf{r})$ of Eq. (4) tends to 1 in the high-density limit, the local hybrid functional uses full exact exchange and treats correlation as the sum of two parts, the static (long-range, left-right) and dynamic (short-range) correlation. The dynamic correlation is relatively easy to model by a semilocal correlation functional $e_c^{\text{sl}}(\mathbf{r})$. The static correlation is represented by the difference $[e_x^{\text{sl}}(\mathbf{r}) - e_x^{\text{ex}}(\mathbf{r})]$ weighted by a position-dependent function $[1 - a(\mathbf{r})]$. This form is motivated by evidence that some (typically more than 100%) of the static correlation is already contained in semilocal exchange approximations [19, 25, 26, 27], but not in $e_x^{\text{ex}}(\mathbf{r})$.

Any proposal for a practical local hybrid functional must deal with the fact that, while the total energy is measurable, physical, and unique, the energy *density* is not. As a result, an arbitrary function $G(\mathbf{r})$ that has a dimension of energy per volume and integrates to zero can be added to any energy density of a global hybrid functional with no effect on the total energy. In contrast, addition of $G(\mathbf{r})$ to $e_x^{\text{ex}}(\mathbf{r})$ or $e_x^{\text{sl}}(\mathbf{r})$ in a local hybrid of Eq. (4) *will* affect the total energy because the exact-exchange energy density here is weighted locally.

While there is no “most correct” choice for the xc-energy density, there is indeed a conventional choice, which for exchange is Eq. (2). However, the conventional exact exchange energy density does not have a second-order gradient expansion [28] and so is not the most natural choice for density-functional approximation. Also, the exchange hole associated with $e_x^{\text{ex}(\text{conv})}$ is highly delocalized, which makes it very difficult to model with semilocal functionals. Standard functionals are at most designed to recover the conventional (or any other) exchange energy density to zeroth-order in the density gradients, i.e., for uniform electron densities only.

In the local hybrids proposed to date [22, 29, 30, 31, 32], $e_x^{\text{sl}}(\mathbf{r})$ is taken as the integrand of the semilocal functional E_x^{sl} as written, while e_x^{ex} is taken as $e_x^{\text{ex}(\text{conv})}$. This choice is not necessarily the one best suited for modeling the static correlation by the difference $(e_x^{\text{sl}} - e_x^{\text{ex}})$. Moreover, the very idea of attaching physical significance to the difference $(e_x^{\text{sl}} - e_x^{\text{ex}})$ requires that both e_x^{sl} and e_x^{ex} be defined with respect to some common reference or gauge.

The choice of the gauge itself is a matter of convention. One such choice is based on the Levy-Perdew virial relation [33]. Burke *et al.* [34] have pointed out that virial exchange energy densities $e_x^{\text{vir}}(\mathbf{r}) = -n(\mathbf{r})\mathbf{r} \cdot \nabla v_x(\mathbf{r})$, where $v_x(\mathbf{r}) = \delta E_x / \delta n(\mathbf{r})$, are unique for any given functional. However, the virial energy density depends on the choice

of origin of \mathbf{r} and has other undesirable properties. Furthermore, for the exact-exchange energy density, this approach requires constructing the optimized effective potential [35, 36] (OEP), a procedure that is problematic in finite basis sets [37, 38, 39]. Burke *et al.* have also proposed [34] and investigated [40] the “unambiguous” exchange-(correlation) energy density which is uniquely determined by the corresponding energy functional via the exchange-(correlation) potential and the Helmholtz theorem. This “unambiguous” exact-exchange energy density has all the desired properties but, like the virial energy density, requires construction of the OEP and, hence, is not very practical at present.

In this work, we propose and implement two new, dependable methods in which $e_x^{\text{sl}}(\mathbf{r})$ serves as the reference and $e_x^{\text{ex}}(\mathbf{r})$ is “tuned” to the gauge of $e_x^{\text{sl}}(\mathbf{r})$. The first of them, summarized in section II A below, is the one we will use in a still-unpublished hyper-GGA [41] based upon the ideas of Ref. [19].

II. THEORY

For a slowly-varying electron density, the conventional exact-exchange energy density will be well approximated by local or semilocal density functionals, although (unlike the integrated exchange energy) it has no analytic gradient expansion [28, 42]. Our idea for making e_x^{ex} compatible with a given e_x^{sl} is based on the observation that although the static correlation is generally quite large (comparable in magnitude to exchange), it is negligible in compact closed systems, such as atoms with nondegenerate electron configurations. Therefore, e_x^{ex} should be close to e_x^{sl} at each \mathbf{r} in such systems. This is consistent with the fact that the conventional exact-exchange [43, 44, 45] or exchange-correlation [46] energy densities in compact closed systems can often be modeled very accurately using only semilocal ingredients.

Hence, we will make e_x^{ex} as close as possible to e_x^{sl} in those systems where the static correlation is known to be small. This can be achieved by various means: for example, by adding to $e_x^{\text{ex}(\text{conv})}$ a term that integrates to zero. We say that the resulting exact-exchange energy density is in the *gauge* of that particular semilocal exchange approximation and denote it by $e_x^{\text{ex}(\text{sl})}$. To illustrate this method, we will construct the exact-exchange energy density in the gauge of the meta-GGA of Tao, Perdew, Staroverov, and Scuseria (TPSS) [8].

A. Construction from the divergence of a vector field

For use as $e_x^{\text{ex}}(\mathbf{r})$ in Eq. (4), we construct the exact-exchange energy density in the gauge of a semilocal functional as follows. First we write

$$e_x^{\text{ex}(\text{sl})}(\mathbf{r}) = e_x^{\text{ex}(\text{conv})}(\mathbf{r}) + G(\mathbf{r}), \quad (5)$$

where $e_x^{\text{ex}(\text{conv})}(\mathbf{r})$ is the conventional exact-exchange energy density given by Eq. (2) and $G(\mathbf{r})$ is the gauge transformation term to be determined, such that

$$\int d\mathbf{r} G(\mathbf{r}) = 0. \quad (6)$$

Obviously, Eq. (6) leaves much freedom in choosing the analytic form of function $G(\mathbf{r})$. The range of possibilities can be narrowed down by several physical considerations: a) $e_x^{\text{ex}(\text{sl})}(\mathbf{r})$ should reproduce $e_x^{\text{sl}}(\mathbf{r})$ in atoms as closely as possible; b) for use in a hyper-GGA, $G(\mathbf{r})$ should contain only the hyper-GGA ingredients, i.e., $n_\sigma(\mathbf{r})$, $\tau_\sigma = \frac{1}{2} \sum_i^{\text{occ.}} |\nabla \phi_{i\sigma}(\mathbf{r})|^2$, $e_{x\sigma}^{\text{ex}(\text{conv})}(\mathbf{r})$, and, possibly, their derivatives; c) $e_x^{\text{ex}(\text{sl})}(\mathbf{r})$ should satisfy as many exact constraints as possible.

We start the construction of $G(\mathbf{r})$ for spin-unpolarized systems by noting that the integral of the divergence of any well-behaved rapidly decaying vector field $\mathbf{F}(\mathbf{r})$ is zero, that is, $\int d\mathbf{r} \nabla \cdot \mathbf{F}(\mathbf{r}) = 0$. So we will take $G(\mathbf{r}) = \nabla \cdot \mathbf{F}(\mathbf{r})$. The vector field $\mathbf{F}(\mathbf{r})$ itself will be chosen from the requirement that $e_x^{\text{ex}(\text{conv})}(\mathbf{r}) + G(\mathbf{r})$ satisfy the most basic properties of the exchange energy density: correct coordinate scaling, finiteness at the nucleus, etc.

One particular form that meets these requirements is:

$$G(\mathbf{r}) = a \nabla \cdot \left[\frac{n/\tilde{\varepsilon}^2}{1 + c(n/\tilde{\varepsilon}^3)^2} \left(\frac{\tau^W}{\tau} \right)^b \nabla \tilde{\varepsilon} \right], \quad (7)$$

where $\tilde{\varepsilon}(\mathbf{r}) = -\varepsilon_x^{\text{ex}(\text{conv})}(\mathbf{r})$, $\tau^W = |\nabla n|^2/8n$ is the von Weizsäcker [47] kinetic energy density for real orbitals, $\tau = \tau_\uparrow + \tau_\downarrow$ is the Kohn-Sham kinetic energy density, and a , b , and c ($c > 0$) are adjustable parameters. Note that $0 \leq \tau^W/\tau \leq 1$ [48].

The function $G(\mathbf{r})$ of Eq. (7) has the following exact properties of the exact-exchange energy density in the conventional gauge (or coordinate-transformed as described in Sec. II B):

(i) Correct uniform coordinate scaling. Under this transformation, the conventional exact-exchange energy density behaves [33] like $e_x^{\text{ex}(\text{conv})}(\mathbf{r}) = \lambda^4 e_x^{\text{ex}(\text{conv})}(\lambda \mathbf{r})$ or, in shorthand, $e_x^{\text{ex}(\text{conv})} \sim \lambda^4$. The ingredients of $G(\mathbf{r})$ behave like $n \sim \lambda^3$, $\tilde{\varepsilon} \sim \lambda$, $\tau^W \sim \lambda^5$, $\tau \sim \lambda^5$, $\nabla \sim \lambda$, so $G_\lambda(\mathbf{r}) = \lambda^4 G(\lambda \mathbf{r})$, which is the correct behavior.

(ii) Correct nonuniform coordinate scaling [49]. Under this scaling, the density behaves like $n_\lambda^x(\mathbf{r}) = \lambda n(\lambda x, y, z)$ or, in shorthand, $n \sim \lambda$. The other ingredients scale in the $\lambda \rightarrow \infty$ limit like $\tilde{\varepsilon} \sim \lambda^0$, $\tau^W \sim \lambda^3$, $\tau \sim \lambda^3$, $\nabla \sim \lambda$, so in this limit $G_\lambda^x(x, y, z) = \lambda G(\lambda x, y, z)$, which is the correct nonuniform coordinate scaling property of the exchange energy density.

(iii) $G(\mathbf{r})$ is finite everywhere. This is because $\tilde{\varepsilon}$ has no cusp at the nucleus [50], which ensures that $\nabla^2 \tilde{\varepsilon}$ is finite. All other ingredients of G are also finite.

(iv) $G(\mathbf{r})$ vanishes for a uniform electron gas and, more generally, satisfies Eq. (6).

We also note that, at large r , the density decays exponentially, $n \sim e^{-\alpha r}$, where α is a constant, $\tau^W/\tau \rightarrow 1$,

$\tilde{\varepsilon} \sim 1/r$, so the large- r behavior is $G(r) \sim -\partial n/\partial r \sim n$, which is comparable to the $-n/2r$ decay of $e_x^{\text{ex}(\text{conv})}$.

The values of a , b , and c are determined by fitting $e_x^{\text{ex}(\text{conv})}(\mathbf{r}) + G(\mathbf{r})$ to $e_x^{\text{sl}}(\mathbf{r})$, where sl=TPSS. In doing so, we note that for one- and closed-shell two-electron (iso-orbital) densities $\tau^W/\tau = 1$, so $G(\mathbf{r})$ is fixed by the parameters a and c alone. We use two model-atom iso-orbital densities: the exact two-electron exponential density $n(r) = (2/\pi)e^{-2r}$ and the two-electron cusplless density $n(r) = (1/2\pi)(1 + 2r)e^{-2r}$. In the case of sl=TPSS, the fit gives $a = 0.015$ and $c = 0.04$. The value $b = 4$ is chosen to be an integer that gives the best fit to the TPSS exchange energy density for the 8-electron jellium cluster with $r_s = 4$ bohr. This choice ensures that $G(\mathbf{r})$ is very small (of the order of ∇^{10}) for a slowly varying density, as it should be. Gauge corrections for semilocal functionals other than TPSS can be constructed similarly by assuming the same analytic form for $G(\mathbf{r})$ and refitting the parameters a , b , and c .

While we cannot rule out that there exists a simpler function $G(\mathbf{r})$ that satisfies exact constraints (i)–(iv), we can point out that many obvious candidates definitely fail to do so. For example, the function $\nabla^2 n^{2/3}$, motivated by the work of Cancio and Chou [46], correctly integrates to zero and has the correct uniform scaling property, but diverges at the nucleus and does not have the proper nonuniform scaling property.

For a partly or fully spin-polarized system, the gauge correction becomes the sum of same-spin contributions $G(\mathbf{r}) = \sum_\sigma G_\sigma(\mathbf{r})$. To deduce the form of $G_\sigma(\mathbf{r})$ we use the spin scaling relation [51]:

$$E_x[n_\uparrow, n_\downarrow] = \frac{1}{2} E_x[2n_\uparrow] + \frac{1}{2} E_x[2n_\downarrow], \quad (8)$$

which also holds for exchange energy densities. Applying Eq. (8) to $G(\mathbf{r})$, we write

$$G([n_\uparrow, n_\downarrow]; \mathbf{r}) = \frac{1}{2} \sum_\sigma G([2n_\sigma]; \mathbf{r}) \quad (9)$$

and define $G_\sigma(\mathbf{r}) \equiv \frac{1}{2} G([2n_\sigma]; \mathbf{r})$. Thus, for spin-polarized systems $G(\mathbf{r}) = \sum_\sigma G_\sigma(\mathbf{r})$, where

$$G_\sigma(\mathbf{r}) = a \nabla \cdot \left[\frac{n_\sigma/\tilde{\varepsilon}_\sigma^2}{1 + 4c(n_\sigma/\tilde{\varepsilon}_\sigma^3)^2} \left(\frac{\tau_\sigma^W}{\tau_\sigma} \right)^b \nabla \tilde{\varepsilon}_\sigma \right], \quad (10)$$

in which $\tau_\sigma^W = |\nabla n_\sigma|^2/8n_\sigma$ and

$$\tilde{\varepsilon}_\sigma = -\varepsilon_{x\sigma}^{\text{ex}(\text{conv})} = -\frac{\varepsilon_{x\sigma}^{\text{ex}(\text{conv})}}{n_\sigma}. \quad (11)$$

Note that $\varepsilon_x^{\text{ex}} \neq \sum_\sigma \varepsilon_{x\sigma}^{\text{ex}}$ but $e_x^{\text{ex}} = \sum_\sigma e_{x\sigma}^{\text{ex}}$ because the spin-scaling relation (8) applies only to energy densities.

B. Construction by a coordinate transformation of the exact-exchange hole

The exact-exchange energy density can be also converted to the gauge of a semilocal approximation by

transforming the exact-exchange hole. The conventional exact-exchange energy density can be written as

$$e_{x\sigma}^{\text{ex(conv)}}(\mathbf{r}) = \frac{n_\sigma(\mathbf{r})}{2} \int d\mathbf{r}' \frac{h_{x\sigma}(\mathbf{r}, \mathbf{r}')}{|\mathbf{r} - \mathbf{r}'|}, \quad (12)$$

where $h_{x\sigma}(\mathbf{r}, \mathbf{r}')$ is the exact-exchange hole

$$h_{x\sigma}(\mathbf{r}, \mathbf{r}') = -\frac{|\gamma_\sigma(\mathbf{r}, \mathbf{r}')|^2}{n_\sigma(\mathbf{r})}, \quad (13)$$

This hole is highly delocalized but can be made less so [52, 53, 54] by an appropriate coordinate transformation $(\mathbf{r}, \mathbf{r}') \rightarrow (\mathbf{r}_1, \mathbf{r}_2)$ of the density matrix, such as [54]

$$\begin{pmatrix} \mathbf{r} \\ \mathbf{r}' \end{pmatrix} = \begin{pmatrix} 2 - \omega & -1 + \omega \\ 1 - \omega & \omega \end{pmatrix} \begin{pmatrix} \mathbf{r}_1 \\ \mathbf{r}_2 \end{pmatrix}, \quad (14)$$

where $0 < \omega < 1$. This transformation does not affect the total exchange energy E_x but yields a distinctly different exchange energy density

$$e_{x\sigma}^{\text{ex}(\omega)}(\mathbf{r}_1) = \frac{n_\sigma(\mathbf{r}_1)}{2} \int d\mathbf{u} \frac{h_{x\sigma}^\omega(\mathbf{r}_1, \mathbf{r}_1 + \mathbf{u})}{u}, \quad (15)$$

where $\mathbf{u} = \mathbf{r}_2 - \mathbf{r}_1$ and $h_{x\sigma}^\omega(\mathbf{r}_1, \mathbf{r}_1 + \mathbf{u})$ is the transformed exact-exchange hole [54]

$$\begin{aligned} h_{x\sigma}^\omega(\mathbf{r}_1, \mathbf{r}_1 + \mathbf{u}) &= h_{x\sigma}(\mathbf{r}_1 + [\omega - 1]\mathbf{u}, \mathbf{r}_1 + \omega\mathbf{u}) \\ &\times \frac{n_\sigma(\mathbf{r}_1 + [\omega - 1]\mathbf{u})}{n_\sigma(\mathbf{r}_1)}, \end{aligned} \quad (16)$$

given in terms of the conventional exchange hole. Since the exchange hole associated with a semilocal functional is relatively local, a transformation of the exact-exchange hole by Eq. (16) can make $e_{x\sigma}^{\text{ex}(\omega)}$ resemble its semilocal approximation more closely than $e_{x\sigma}^{\text{ex(conv)}}$ does. It should be noted that the transformed hole of Eq. (15) does not obey the sum rule for the conventional hole at each \mathbf{r}_1 , but preserves the correct normalization of the system-averaged exchange hole [54].

The extent of locality of the exchange hole depends on the value of parameter ω . The maximal localization is achieved at $\omega = 1/2$ [54, 55]. We have numerically evaluated the transformed exact-exchange energy density $e_{x\sigma}^{\text{ex}(\omega)}(\mathbf{r})$ for various values of ω and found that $\omega = 0.92$ leads to the best fit of the exact-exchange energy density to the TPSS meta-GGA.

III. COMPUTATIONAL METHODOLOGY

In practice, it is much easier to construct the gauge correction function $G(\mathbf{r})$ than to perform numerical integration over transformed coordinates of the exchange hole in Eq. (15). Therefore, we will adopt the former method for the purpose of constructing a hyper-GGA functional. In this section, we describe a general-purpose implementation of the TPSS gauge term $G(\mathbf{r})$ in finite basis sets.

A. Evaluation of the exact-exchange energy density in the conventional gauge

Analytic evaluation of the conventional exact-exchange energy density by Eqs. (2) and (3) is possible but impractical because it requires evaluation and contraction of many one-electron integrals for each grid point \mathbf{r} . Instead, we employ a much more efficient approximate method of Della Sala and Görling [56]. Although this method is documented in the literature [29, 56], we will supply its detailed derivation here because it serves as a stepping-stone for evaluating our function $G(\mathbf{r})$.

When a basis set $\{\chi_\mu\}$ is introduced, each Kohn-Sham orbital is taken as a linear combination of one-electron basis functions, $\phi_{i\sigma}(\mathbf{r}) = \sum_\mu c_{\mu i}^\sigma \chi_\mu(\mathbf{r})$. In terms of these basis functions, the density matrix of Eq. (3) is

$$\gamma_\sigma(\mathbf{r}, \mathbf{r}') = \sum_{\mu\nu} P_{\mu\nu}^\sigma \chi_\mu(\mathbf{r}) \chi_\nu^*(\mathbf{r}'), \quad (17)$$

where $P_{\mu\nu}^\sigma = P_{\nu\mu}^\sigma = \sum_i^{\text{occ.}} c_{\mu i}^\sigma (c_{\nu i}^\sigma)^*$. The conventional exact-exchange energy density of Eq. (2) can be written as

$$\begin{aligned} e_{x\sigma}^{\text{ex(conv)}}(\mathbf{r}) &= -\frac{1}{2} \sum_{\eta\kappa} \sum_{\rho\nu} \int d\mathbf{r}' P_{\eta\kappa}^\sigma P_{\rho\nu}^\sigma \\ &\times \frac{\chi_\eta(\mathbf{r}) \chi_\nu^*(\mathbf{r}) \chi_\rho(\mathbf{r}') \chi_\kappa^*(\mathbf{r}')}{|\mathbf{r} - \mathbf{r}'|}. \end{aligned} \quad (18)$$

The single integral over \mathbf{r}' in Eq. (18) is not so easily evaluated for many different values of \mathbf{r} , but introducing a second integration over \mathbf{r} yields $E_{x\sigma}^{\text{ex}}$, which is evaluated analytically and simply in Gaussian basis sets. These facts motivate the following development. Using the δ -function one can write

$$\frac{\chi_\eta(\mathbf{r})}{|\mathbf{r} - \mathbf{r}'|} = \int d\mathbf{r}'' \frac{\chi_\eta(\mathbf{r}'')}{|\mathbf{r}'' - \mathbf{r}'|} \delta(\mathbf{r}'' - \mathbf{r}). \quad (19)$$

The δ -function can be approximated by an expansion in the same non-orthogonal basis as the orbitals, namely, $\delta(\mathbf{r}'' - \mathbf{r}) = \sum_\mu \chi_\mu(\mathbf{r}) c_\mu(\mathbf{r}'')$, whose Fourier coefficients $c_\mu(\mathbf{r}')$ can be determined as usual. This yields

$$\delta(\mathbf{r}'' - \mathbf{r}) = \sum_{\mu\xi} \chi_\mu(\mathbf{r}) S_{\mu\xi}^{-1} \chi_\xi^*(\mathbf{r}''), \quad (20)$$

where $S_{\mu\xi}^{-1}$ are matrix elements of the inverse of the basis set overlap matrix. Substitution of Eqs. (19) and (20) into Eq. (18) gives

$$e_{x\sigma}^{\text{ex(conv)}}(\mathbf{r}) = \frac{1}{2} \sum_{\rho\nu} \sum_{\mu\xi} S_{\mu\xi}^{-1} K_{\xi\rho}^\sigma P_{\rho\nu}^\sigma \chi_\mu(\mathbf{r}) \chi_\nu^*(\mathbf{r}), \quad (21)$$

where

$$K_{\xi\rho}^\sigma = -\sum_{\eta\kappa} P_{\eta\kappa}^\sigma \int d\mathbf{r}' \int d\mathbf{r}'' \frac{\chi_\rho(\mathbf{r}') \chi_\kappa^*(\mathbf{r}') \chi_\eta(\mathbf{r}'') \chi_\xi^*(\mathbf{r}'')}{|\mathbf{r}'' - \mathbf{r}'|} \quad (22)$$

are elements of the exchange matrix. Eq. (21) can be rewritten as

$$e_{x\sigma}^{\text{ex(conv)}}(\mathbf{r}) = \frac{1}{2} \sum_{\mu\nu} \tilde{Q}_{\mu\nu}^{\sigma} \chi_{\mu}(\mathbf{r}) \chi_{\nu}^*(\mathbf{r}), \quad (23)$$

where $\tilde{Q}_{\mu\nu}^{\sigma}$ are elements of the matrix $\tilde{\mathbf{Q}}^{\sigma} = \mathbf{S}^{-1} \mathbf{K}^{\sigma} \mathbf{P}^{\sigma}$. Eq. (23) is analogous to the formula for the density $n(\mathbf{r}) \equiv \gamma_{\sigma}(\mathbf{r}, \mathbf{r}) = \sum_{\mu\nu} P_{\mu\nu}^{\sigma} \chi_{\mu}(\mathbf{r}) \chi_{\nu}^*(\mathbf{r})$ except that, unlike \mathbf{P}^{σ} , the matrix $\tilde{\mathbf{Q}}^{\sigma}$ is generally not symmetric. The analogy can be made complete by replacing $\tilde{\mathbf{Q}}^{\sigma}$ with the symmetrized matrix

$$\mathbf{Q}^{\sigma} = \frac{1}{2} (\mathbf{P}^{\sigma} \mathbf{K}^{\sigma} \mathbf{S}^{-1} + \mathbf{S}^{-1} \mathbf{K}^{\sigma} \mathbf{P}^{\sigma}). \quad (24)$$

The final formula for the conventional exact-exchange energy density via the resolution of the identity is

$$e_{x\sigma}^{\text{ex(conv)}}(\mathbf{r}) = \frac{1}{2} \sum_{\mu\nu} Q_{\mu\nu}^{\sigma} \chi_{\mu}(\mathbf{r}) \chi_{\nu}^*(\mathbf{r}). \quad (25)$$

In practice, $e_{x\sigma}^{\text{ex(conv)}}$ is computed using the subroutines that evaluate $n(\mathbf{r})$ by passing $\frac{1}{2} \mathbf{Q}^{\sigma}$ in place of \mathbf{P}^{σ} .

B. Evaluation of the exact-exchange energy density in the TPSS gauge

The exact-exchange energy density in the TPSS gauge is given by Eq. (5). The first term, $e_{x\sigma}^{\text{ex(conv)}}(\mathbf{r})$, is computed by Eq. (25) and the gauge term is evaluated as follows. Let us rewrite Eq. (10) as

$$G_{\sigma}(\mathbf{r}) = a [\nabla f_{\sigma}(\mathbf{r}) \cdot \nabla \tilde{\varepsilon}_{\sigma}(\mathbf{r}) + f_{\sigma}(\mathbf{r}) \nabla^2 \tilde{\varepsilon}_{\sigma}(\mathbf{r})], \quad (26)$$

where

$$f_{\sigma}(\mathbf{r}) = \frac{n_{\sigma} / \tilde{\varepsilon}_{\sigma}^2}{1 + 4c (n_{\sigma} / \tilde{\varepsilon}_{\sigma}^3)^2} \left(\frac{\tau_{\sigma}^W}{\tau_{\sigma}} \right)^b. \quad (27)$$

Based on Eq. (11),

$$\nabla \tilde{\varepsilon}_{\sigma} = - \frac{\nabla e_{x\sigma}^{\text{ex(conv)}} + \tilde{\varepsilon}_{\sigma} \nabla n_{\sigma}}{n_{\sigma}}, \quad (28)$$

$$\nabla^2 \tilde{\varepsilon}_{\sigma} = - \frac{\nabla^2 e_{x\sigma}^{\text{ex(conv)}} + 2 \nabla \tilde{\varepsilon}_{\sigma} \cdot \nabla n_{\sigma} + \tilde{\varepsilon}_{\sigma} \nabla^2 n_{\sigma}}{n_{\sigma}}. \quad (29)$$

Eqs. (28) and (29) involve the first and second derivatives of the exact-exchange energy density in the conventional gauge. These quantities are computed as

$$\nabla e_{x\sigma}^{\text{ex(conv)}} = \frac{1}{2} \sum_{\mu\nu} Q_{\mu\nu}^{\sigma} \nabla [\chi_{\mu}(\mathbf{r}) \chi_{\nu}^*(\mathbf{r})], \quad (30)$$

$$\nabla^2 e_{x\sigma}^{\text{ex(conv)}} = \frac{1}{2} \sum_{\mu\nu} Q_{\mu\nu}^{\sigma} \nabla^2 [\chi_{\mu}(\mathbf{r}) \chi_{\nu}^*(\mathbf{r})], \quad (31)$$

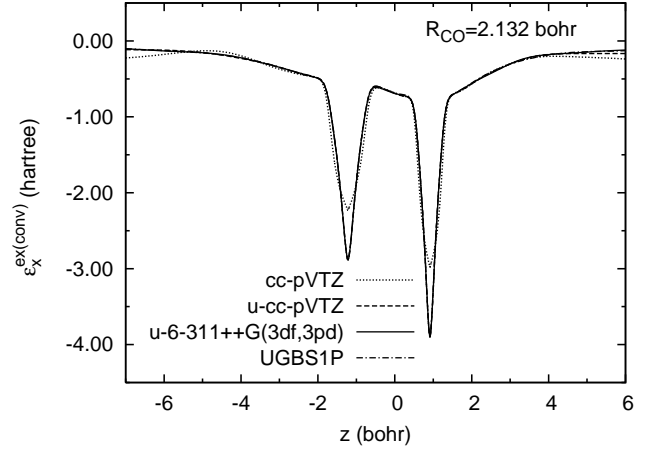


FIG. 1: Conventional exact-exchange energy per electron in the CO molecule along the internuclear axis evaluated at the experimental geometry using the approximate resolution of the identity in four basis sets. The curves for the last three basis sets are close together everywhere.

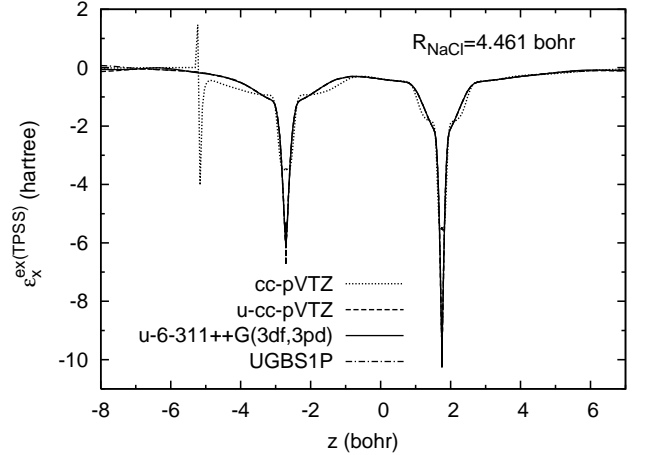


FIG. 2: Exact-exchange energy per electron in the TPSS gauge in the NaCl molecule evaluated at the experimental geometry using the approximate resolution of the identity in four basis sets. The curves for the last three basis sets are almost indistinguishable.

using the same subroutines that evaluate $\nabla n_{\sigma}(\mathbf{r})$ and $\nabla^2 n_{\sigma}(\mathbf{r})$ by passing $\frac{1}{2} \mathbf{Q}^{\sigma}$ instead of \mathbf{P}^{σ} . Note that Eq. (21) clearly shows that matrix elements $Q_{\mu\nu}^{\sigma}$ themselves do not depend on \mathbf{r} .

The gradient $\nabla f_{\sigma}(\mathbf{r})$ can be written as

$$\nabla f_{\sigma}(\mathbf{r}) = \left(\frac{\tau_{\sigma}^W}{\tau_{\sigma}} \right)^b \nabla g_{\sigma}(\mathbf{r}) + g_{\sigma}(\mathbf{r}) \nabla \left(\frac{\tau_{\sigma}^W}{\tau_{\sigma}} \right)^b, \quad (32)$$

where

$$g_{\sigma}(\mathbf{r}) = \frac{n_{\sigma} \tilde{\varepsilon}_{\sigma}^4}{\tilde{\varepsilon}_{\sigma}^6 + 4cn_{\sigma}^2}. \quad (33)$$

The quantity $\nabla g_{\sigma}(\mathbf{r})$ is evaluated using the chain rule as

usual and it involves only the first derivatives of $n(\mathbf{r})$ and $e_{x\sigma}^{\text{ex(conv)}}(\mathbf{r})$. The second term can be written as

$$\nabla \left(\frac{\tau_\sigma^W}{\tau_\sigma} \right)^b = b \left(\frac{\tau_\sigma^W}{\tau_\sigma} \right)^b \left(\frac{\nabla \tau_\sigma^W}{\tau_\sigma^W} - \frac{\nabla \tau_\sigma}{\tau_\sigma} \right). \quad (34)$$

The gradient $\nabla \tau_\sigma^W$ involves derivatives of the type

$$\frac{\partial |\nabla n_\sigma|^2}{\partial x} = 2 \left(\frac{\partial n_\sigma}{\partial x} \frac{\partial^2 n_\sigma}{\partial x^2} + \frac{\partial n_\sigma}{\partial y} \frac{\partial^2 n_\sigma}{\partial y \partial x} + \frac{\partial n_\sigma}{\partial z} \frac{\partial^2 n_\sigma}{\partial z \partial x} \right) \quad (35)$$

and similar expressions for $\partial |\nabla n_\sigma|^2 / \partial y$ and $\partial |\nabla n_\sigma|^2 / \partial z$. Finally, the gradient of the Kohn-Sham kinetic energy density $\nabla \tau_\sigma$ has the components

$$\frac{\partial \tau_\sigma}{\partial x} = \sum_i^{\text{occ.}} \left(\frac{\partial \phi_{i\sigma}}{\partial x} \frac{\partial^2 \phi_{i\sigma}}{\partial x^2} + \frac{\partial \phi_{i\sigma}}{\partial y} \frac{\partial^2 \phi_{i\sigma}}{\partial y \partial x} + \frac{\partial \phi_{i\sigma}}{\partial z} \frac{\partial^2 \phi_{i\sigma}}{\partial z \partial x} \right) \quad (36)$$

and similarly for $\partial \tau_\sigma / \partial y$ and $\partial \tau_\sigma / \partial z$.

The quantities given by Eqs. (35) and (36) are not used in any of the common GGA and meta-GGA functionals and may not be immediately available in standard density functional codes. However, the first and second derivatives of the orbitals, from which Eqs. (35) and (36) are built, are readily available. Thus, evaluation of the exact-exchange energy density and the gauge correction requires some modification of existing subroutines. We have implemented these formulas in a development version of the GAUSSIAN program [57].

C. Basis set effects

We use the same nonorthogonal basis set $\{\chi_\mu\}$ to expand the Kohn-Sham orbitals and to approximate the δ -function by Eq. (20). Since Eq. (20) in a finite basis set is not exact, the conventional exact-exchange energy density $e_x^{\text{ex(conv)}}$ and its derivatives are only approximate when evaluated by Eqs. (25), (30), and (31). In fact, small and medium-size contracted basis sets may cause large errors in $e_x^{\text{ex(conv)}}$ that are further magnified in $e_x^{\text{ex(TPSS)}}$ via $\nabla e_x^{\text{ex(conv)}}$ and $\nabla^2 e_x^{\text{ex(conv)}}$. Figs. 1 and 2 show that, for instance, the cc-pVTZ basis is insufficiently flexible. On the other hand, the uncontracted cc-pVTZ basis set works almost as well as the near-complete UGBS1P basis [58, 59]. In general, uncontracted basis sets work much better in resolution of the identity techniques than the corresponding contracted bases.

Furthermore, when cuspless Gaussian-type basis functions are used, $|\nabla n_\sigma|^2$ and $|\nabla \tau_\sigma|^2$ exhibit spurious oscillations in the vicinity of a nucleus. However, these artifacts are common to all semilocal density functional calculations employing Gaussian-type orbitals, are negligible energetically and may be ignored.

In summary, we caution against using medium-size contracted basis sets like cc-pVTZ or 6-311+G* in Eqs. (25), (30), and (31). When in doubt, it is always

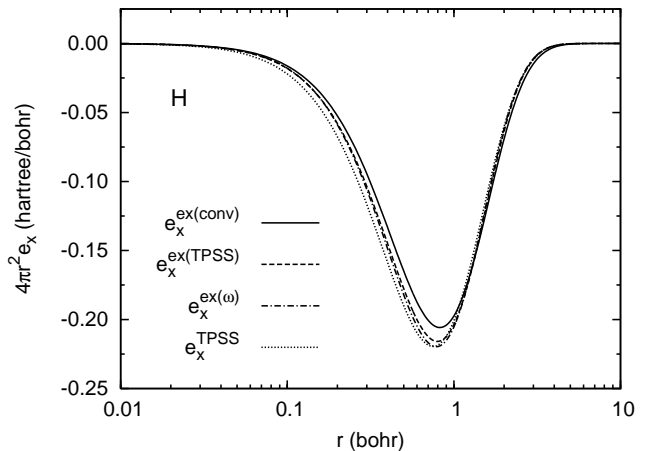


FIG. 3: Radial exchange energy densities of the H atom computed at the exact ground-state density: exact conventional [ex(conv)], exact in the TPSS gauge [ex(TPSS)], exact from a transformed exchange hole [ex(ω), $\omega = 0.92$], and TPSS.

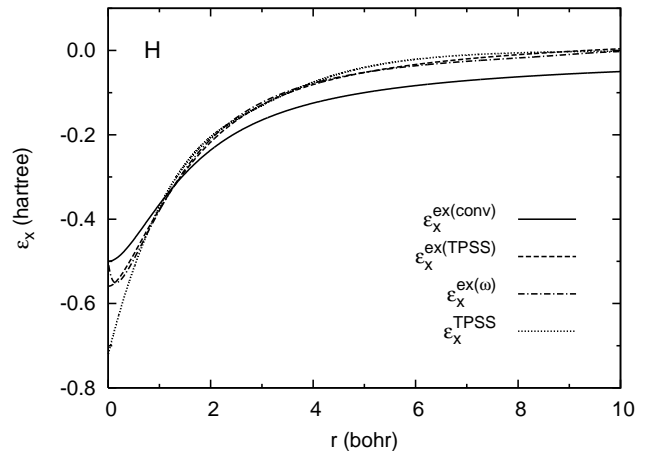


FIG. 4: Exchange energies per electron in the H atom computed at the exact ground-state density. For the explanation of the legend, refer to Fig. 3.

safer to uncontract the basis set. In particular, we recommend the fully uncontracted 6-311++G(3df,3pd) basis set, denoted as u-6-311++G(3df,3pd), which strikes perfect balance between accuracy and computational cost.

IV. RESULTS

The fact that the TPSS meta-GGA was designed to recover many exact properties [8, 10] of the exact-exchange functional does not guarantee that e_x^{TPSS} is close to $e_x^{\text{ex(conv)}}$. This is evident from Fig. 3 which shows radial plots of these energy densities in the H atom. The TPSS and conventional exact-exchange energy density are different, even though they both integrate to the same exact value of $-5/16$ hartree [8]. The exact-exchange energy

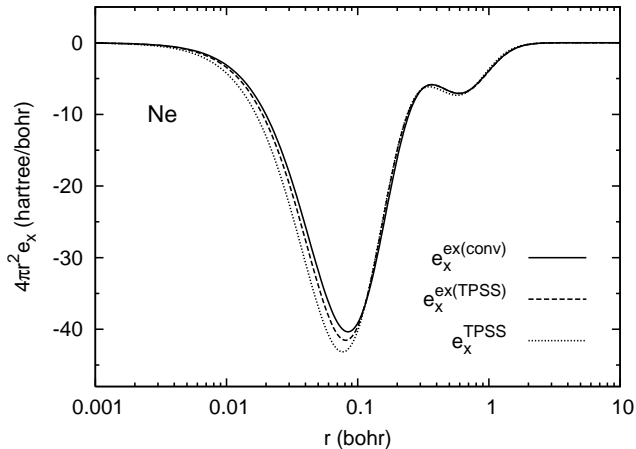


FIG. 5: Radial exchange energy densities of the Ne atom computed at the converged Hartree-Fock orbitals in the UGBS basis set: exact conventional [ex(conv)], exact in the TPSS gauge [ex(TPSS)], and semilocal TPSS approximation.

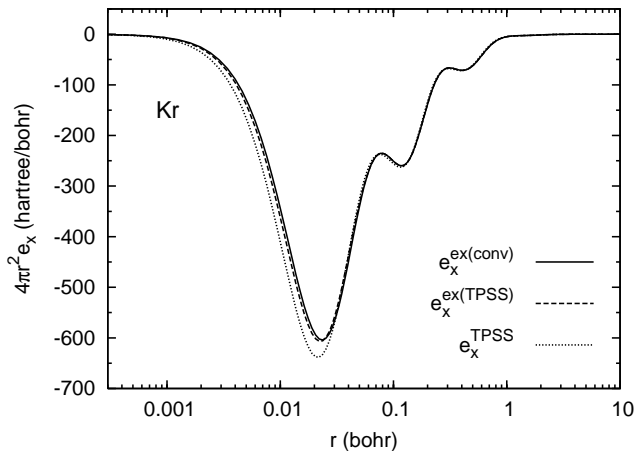


FIG. 6: Same as in Fig. 5 for the Kr atom.

densities in the TPSS gauge $e_x^{\text{ex(TPSS)}}$ and $e_x^{\text{ex}(\omega)}$ are both much closer than $e_x^{\text{ex(conv)}}$ to the semilocal e_x^{TPSS} .

Fig. 4 shows the exchange energy per electron, $\varepsilon_x = e_x/n$ vs. n for the H atom, comparing the exact conventional, exact in the TPSS gauge, and the hole-transformed ($\omega = 0.92$) exact-exchange energies per electron to the semilocal TPSS exchange approximation. Unlike Fig. 3, this figure shows what happens in the energetically unimportant small- r and large- r regions. The transformed exact-exchange energy per electron $\varepsilon_x^{\text{ex}(\omega)}$ stands apart from the others in that it appears to have an inverted cusp at the nucleus.

Figs. 5 and 6 compare exchange energy in the Ne and Kr atoms evaluated in a post-self-consistent manner at the converged Hartree-Fock orbitals obtained using the near-complete UGBS basis set [58]. Overall, Figs. 3–6 suggest that, for the smaller atoms, the exact-exchange

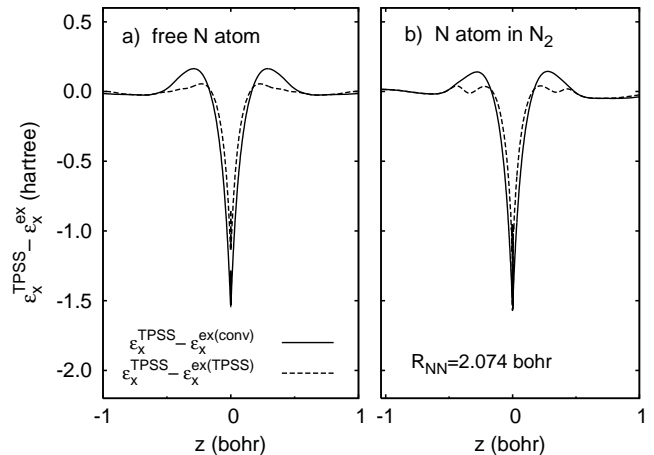


FIG. 7: Difference $\varepsilon_x^{\text{TPSS}} - \varepsilon_x^{\text{ex}}$, where $\varepsilon_x^{\text{ex}}$ is in the conventional and TPSS gauges, in a free N atom and along the internuclear axis of the N_2 molecule at the experimental geometry. Panel b) shows only the right half of the molecule with the N nucleus placed at $z = 0$. All quantities were computed at the converged TPSS orbitals using the UGBS1P basis set.

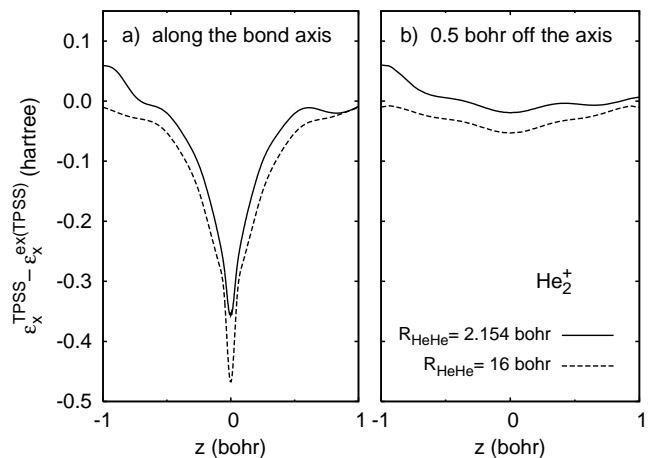


FIG. 8: Difference $\varepsilon_x^{\text{TPSS}} - \varepsilon_x^{\text{ex(TPSS)}}$ in the He_2^+ molecule along the internuclear axis and along a parallel axis offset by 0.5 bohr. Each panel shows only the region near the right nucleus which is always placed at $z = 0$. The static correlation in the stretched molecule $\text{He}^{0.5+} \dots \text{He}^{0.5+}$ (dashed line) is more negative than at the equilibrium TPSS/cc-pVQZ geometry (solid line). All quantities were computed at the converged TPSS orbitals using the uncontracted cc-pVQZ basis set.

energy density in the TPSS gauge is closer than $e_x^{\text{ex(conv)}}$ to the TPSS exchange energy density. For larger atoms, however, $e_x^{\text{ex(TPSS)}}$ remains closer to $e_x^{\text{ex(conv)}}$ than to e_x^{TPSS} in the deep core region.

Fig. 7 shows that the exact-exchange energy density (per electron) in the gauge of a semilocal approximation, $\varepsilon_x^{\text{ex(TPSS)}}$, differs from $\varepsilon_x^{\text{ex(conv)}}$ in a non-trivial way. The difference $\varepsilon_x^{\text{TPSS}} - \varepsilon_x^{\text{ex(TPSS)}}$ reveals subtle effects in the N_2 molecule that are absent in a free N atom. Off-axis

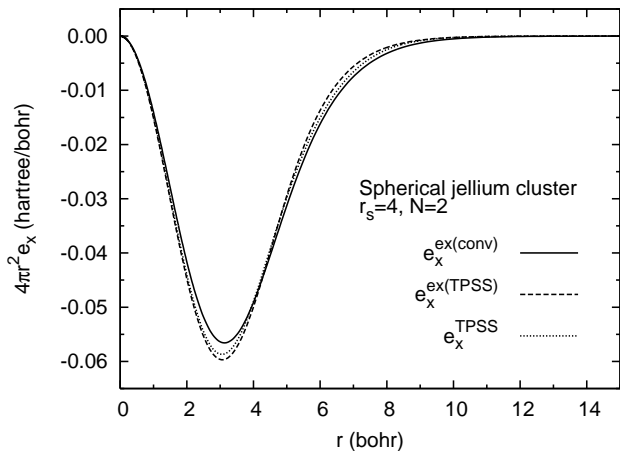


FIG. 9: Radial exchange energy densities for a spherical jellium cluster of $N = 2$ electrons computed at the exchange-only OEP orbitals: exact conventional [ex(conv)], exact in the TPSS gauge [ex(TPSS)], and semilocal (TPSS).

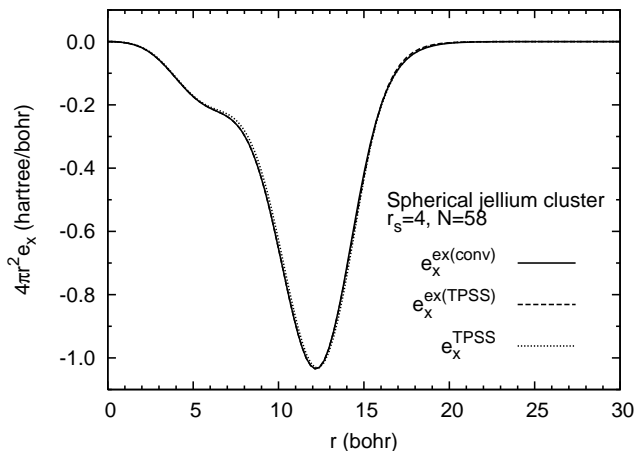


FIG. 10: Same as in Fig. 9 for a cluster of $N = 58$ electrons.

effects (not shown) are of course important. In contrast, the difference $\varepsilon_x^{\text{TPSS}} - \varepsilon_x^{\text{ex(conv)}}$ in the N_2 molecule is very similar to that in a free N atom.

Fig. 8 shows that the difference $\varepsilon_x^{\text{TPSS}} - \varepsilon_x^{\text{ex(TPSS)}}$ representing the static correlation gets substantially more negative upon bond stretching, when the fragments show large fluctuations of electron number at the Hartree-Fock level, as it should. Note that the nuclei in the stretched He_2^+ molecule ($R_{\text{HeHe}} = 16$ bohr) are essentially isolated, so the difference $\varepsilon_x^{\text{TPSS}} - \varepsilon_x^{\text{ex(TPSS)}}$ is almost perfectly symmetric about $z = 0$.

We have also evaluated the exact-exchange energy density in the TPSS gauge and the two conventional energy densities for spherical jellium clusters. A spherical jellium cluster is a model system that has a uniform positive background charge and a spherically distributed electron density. The radius of the sphere is given by

$R = r_s N^{1/3}$, where r_s is the bulk density parameter and N is the number of electrons in the system. The volume of sphere is proportional to N and is given by the relation $V = (4\pi/3)Nr_s^3$. The three exchange energy densities for the jellium clusters of $r_s = 4$ for $N = 2$ and 58 are shown in Figs. 9 and 10. All three quantities, $e_x^{\text{ex(conv)}}$, $e_x^{\text{ex(TPSS)}}$, and e_x^{TPSS} , were evaluated at the orbitals and densities obtained from OEP calculations [35, 36, 60]. As with atoms and molecules, $e_x^{\text{ex(TPSS)}}$ is closer than $e_x^{\text{ex(conv)}}$ to e_x^{TPSS} in these jellium clusters.

V. CONCLUSION

As observed before [43, 44, 45], the exchange energy density of a semilocal functional is reasonably close to the conventional exact-exchange energy density of Eq. (2) in compact systems like atoms or spherical jellium clusters. We confirm this here for the nonempirical TPSS meta-GGA. The relative differences are largest in regions of space where the density is dominated by a single orbital shape, making τ^W/τ close to 1, e.g., the H or He atoms and the two-electron jellium cluster. Particularly in these regions, the difference can be reduced by a gauge transformation of the conventional exact-exchange energy density.

We have found a simple, realistic, and not too highly parametrized form of the function $G(\mathbf{r})$, given by Eq. (7), which via Eq. (5) transforms the conventional difference of semilocal and exact-exchange energy densities appearing in Eq. (4) to the gauge of the TPSS meta-GGA. This transformation solves the problem of nonuniqueness of the exact-exchange energy density arising in the context of modeling the static correlation by the difference of semilocal and exact exchange energy densities. The transformed exact-exchange energy density $e_x^{\text{ex(TPSS)}}$ does in fact contain more information about electron correlation than $e_x^{\text{ex(conv)}}$. In a forthcoming article [41], we will present a construction of a hyper-GGA that relies on this gauge transformation to give highly accurate thermochemistry and reaction barriers.

Finally, we have demonstrated that, as expected [19], the difference between semilocal and exact-exchange energy densities becomes more negative under bond stretching in He_2^+ and related systems, where the separating fragments show large fluctuations of electron number at the independent-electron level.

Acknowledgments

This work was supported by the NSF under Grants DMR-0501588 (J.T. and J.P.P.) and CHE-0457030 (V.N.S. and G.E.S.), by DOE under Contract No. DE-AC52-06NA25396 and the LDRD programs at LANL (J.T.), and by the NSERC of Canada (V.N.S.)

-
- [1] W. Kohn and L. J. Sham, *Phys. Rev.* **140**, A1133 (1965).
- [2] C. Fiolhais, F. Nogueira, and M. Marques, eds., *A Primer in Density Functional Theory* (Springer, Berlin, 2003).
- [3] J. P. Perdew and K. Schmidt, in *Density Functional Theory and Its Application to Materials*, edited by V. Van Doren, C. Van Alsenoy, and P. Geerlings (AIP, Melville, NY, 2001).
- [4] J. P. Perdew, A. Ruzsinszky, J. Tao, V. N. Staroverov, G. E. Scuseria, and G. I. Csonka, *J. Chem. Phys.* **123**, 062201 (2005).
- [5] S. H. Vosko, L. Wilk, and M. Nusair, *Can. J. Phys.* **58**, 1200 (1980).
- [6] J. P. Perdew and Y. Wang, *Phys. Rev. B* **45**, 13244 (1992).
- [7] J. P. Perdew, K. Burke, and M. Ernzerhof, *Phys. Rev. Lett.* **77**, 3865 (1996); **78**, 1396(E) (1997).
- [8] J. Tao, J. P. Perdew, V. N. Staroverov, and G. E. Scuseria, *Phys. Rev. Lett.* **91**, 146401 (2003).
- [9] V. N. Staroverov, G. E. Scuseria, J. Tao, and J. P. Perdew, *J. Chem. Phys.* **119**, 12129 (2003); **121**, 11507(E) (2004).
- [10] V. N. Staroverov, G. E. Scuseria, J. Tao, and J. P. Perdew, *Phys. Rev. B* **69**, 075102 (2004).
- [11] G. I. Csonka, A. Ruzsinszky, J. Tao, and J. P. Perdew, *Int. J. Quantum Chem.* **101**, 506 (2005).
- [12] J. Tao, J. P. Perdew, A. Ruzsinszky, G. E. Scuseria, G. I. Csonka, and V. N. Staroverov, *Philos. Mag.* **87**, 1071 (2007).
- [13] F. Furche and J. P. Perdew, *J. Chem. Phys.* **124**, 044103 (2006).
- [14] J. P. Perdew, in *Density Functional Methods in Physics*, edited by R. M. Dreizler and J. da Providência (Plenum, New York, 1985).
- [15] J. P. Perdew, *Adv. Quantum Chem.* **21**, 113 (1990).
- [16] P. Mori-Sánchez, A. J. Cohen, and W. Yang, *J. Chem. Phys.* **125**, 201102 (2006).
- [17] A. Ruzsinszky, J. P. Perdew, G. I. Csonka, O. A. Vydrov, and G. E. Scuseria, *J. Chem. Phys.* **126**, 104102 (2007).
- [18] O. A. Vydrov, G. E. Scuseria, and J. P. Perdew, *J. Chem. Phys.* **126**, 154109 (2007).
- [19] J. P. Perdew, A. Ruzsinszky, G. I. Csonka, O. A. Vydrov, G. E. Scuseria, V. N. Staroverov, and J. Tao, *Phys. Rev. A* **76**, 040501(R) (2007).
- [20] A. D. Becke, *J. Chem. Phys.* **98**, 5648 (1993).
- [21] F. G. Cruz, K.-C. Lam, and K. Burke, *J. Phys. Chem. A* **102**, 4911 (1998).
- [22] J. Jaramillo, G. E. Scuseria, and M. Ernzerhof, *J. Chem. Phys.* **118**, 1068 (2003).
- [23] A. D. Becke, *J. Chem. Phys.* **122**, 064101 (2005).
- [24] P. Mori-Sánchez, A. J. Cohen, and W. Yang, *J. Chem. Phys.* **124**, 091102 (2006).
- [25] P. R. T. Schipper, O. V. Gritsenko, and E. J. Baerends, *Phys. Rev. A* **57**, 1729 (1998).
- [26] N. C. Handy and A. J. Cohen, *Mol. Phys.* **99**, 403 (2001).
- [27] K. Molawi, A. J. Cohen, and N. C. Handy, *Int. J. Quantum Chem.* **89**, 86 (2002).
- [28] R. Armiento and A. E. Mattsson, *Phys. Rev. B* **66**, 165117 (2002).
- [29] A. V. Arbuznikov, M. Kaupp, and H. Bahmann, *J. Chem. Phys.* **124**, 204102 (2006).
- [30] H. Bahmann, A. Rodenberg, A. V. Arbuznikov, and M. Kaupp, *J. Chem. Phys.* **126**, 011103 (2007).
- [31] A. V. Arbuznikov and M. Kaupp, *Chem. Phys. Lett.* **440**, 160 (2007).
- [32] B. G. Janesko and G. E. Scuseria, *J. Chem. Phys.* **127**, 164117 (2007).
- [33] M. Levy and J. P. Perdew, *Phys. Rev. A* **32**, 2010 (1985).
- [34] K. Burke, F. G. Cruz, and K.-C. Lam, *J. Chem. Phys.* **109**, 8161 (1998).
- [35] J. D. Talman and W. F. Shadwick, *Phys. Rev. A* **14**, 36 (1976).
- [36] S. Kümmel and J. P. Perdew, *Phys. Rev. Lett.* **90**, 043004 (2003).
- [37] V. N. Staroverov, G. E. Scuseria, and E. R. Davidson, *J. Chem. Phys.* **124**, 141103 (2006).
- [38] V. N. Staroverov, G. E. Scuseria, and E. R. Davidson, *J. Chem. Phys.* **125**, 081104 (2006).
- [39] A. F. Izmaylov, V. N. Staroverov, G. E. Scuseria, and E. R. Davidson, *J. Chem. Phys.* **127**, 084113 (2007).
- [40] K. Burke, F. G. Cruz, and K.-C. Lam, *Int. J. Quantum Chem.* **70**, 583 (1998).
- [41] J. P. Perdew, V. N. Staroverov, G. E. Scuseria, and J. Tao, work in progress.
- [42] J. P. Perdew and Y. Wang, in *Mathematics Applied to Science*, edited by J. A. Goldstein, S. Rosencrans, and G. A. Sod (Academic Press, Boston, 1988).
- [43] N. O. Folland, *Phys. Rev. A* **3**, 1535 (1971).
- [44] A. D. Becke, *Phys. Rev. A* **38**, 3098 (1988).
- [45] J. Tao, *J. Chem. Phys.* **115**, 3519 (2001).
- [46] A. C. Cancio and M. Y. Chou, *Phys. Rev. B* **74**, 081202(R) (2006).
- [47] C. F. von Weizsäcker, *Z. Phys.* **96**, 431 (1935).
- [48] S. Kurth, J. P. Perdew, and P. Blaha, *Int. J. Quantum Chem.* **75**, 889 (1999).
- [49] M. Levy, *Phys. Rev. A* **43**, 4637 (1991).
- [50] N. H. March, I. A. Howard, A. Holas, P. Senet, and V. E. Van Doren, *Phys. Rev. A* **63**, 012520 (2000).
- [51] G. L. Oliver and J. P. Perdew, *Phys. Rev. A* **20**, 397 (1979).
- [52] R. M. Koehl, G. K. Odom, and G. E. Scuseria, *Mol. Phys.* **87**, 835 (1996).
- [53] M. Springborg, *Chem. Phys. Lett.* **308**, 83 (1999).
- [54] J. Tao, M. Springborg, and J. P. Perdew, *J. Chem. Phys.* **119**, 6457 (2003).
- [55] M. Springborg, J. P. Perdew, and K. Schmidt, *Z. Phys. Chem.* **215**, 1243 (2001).
- [56] F. Della Sala and A. Görling, *J. Chem. Phys.* **115**, 5718 (2001).
- [57] M. J. Frisch *et al.*, Gaussian Development Version, Revision D.01+, Gaussian, Inc., Wallingford, CT, 2004.
- [58] E. V. R. de Castro and F. E. Jorge, *J. Chem. Phys.* **108**, 5225 (1998).
- [59] A. Frisch, M. J. Frisch, and G. W. Trucks, *Gaussian 03 User's Reference* (Wallingford, CT, 2005), 2nd ed.
- [60] E. Engel and R. M. Dreizler, *J. Comput. Chem.* **20**, 31 (1999).